


RESEARCH PAPER

# Correlation and co-localization of QTL for stomatal density, canopy temperature, and productivity with and without drought stress in *Setaria*

Parthiban Thathapalli Prakash<sup>1,2,\*</sup>, Darshi Banan<sup>2,3</sup>, Rachel E. Paul<sup>2,3</sup>, Maximilian J. Feldman<sup>4</sup>, Dan Xie<sup>2,3,†</sup>, Luke Freyfogle<sup>2,3</sup>, Ivan Baxter<sup>5</sup>  and Andrew D.B. Leakey<sup>1,2,3,‡</sup> 

<sup>1</sup> Department of Crop Sciences, University of Illinois at Urbana-Champaign, Urbana, IL 61801, USA

<sup>2</sup> Institute for Genomic Biology, University of Illinois at Urbana-Champaign, Urbana, IL 61801, USA

<sup>3</sup> Department of Plant Biology, University of Illinois at Urbana-Champaign, Urbana, IL 61801, USA

<sup>4</sup> USDA-ARS, 24106 N Bunn Rd, Prosser, WA 99350, USA

<sup>5</sup> Donald Danforth Plant Science Center, 975 North Warson Road, St Louis, MO 63132, USA

\* International Rice Research Institute, Los Baños, Philippines.

† Department of Medicinal Chemistry and Molecular Pharmacology, Purdue University, West Lafayette, IN 47907, USA.

Present address:

‡ Correspondence: [leakey@illinois.edu](mailto:leakey@illinois.edu)

Received 14 October 2020; Editorial decision 12 April 2021; Accepted 23 April 2021

Editor: Tracy Lawson, University of Essex, UK

## Abstract

**Mechanistic modeling indicates that stomatal conductance could be reduced to improve water use efficiency (WUE) in *C*<sub>4</sub> crops. Genetic variation in stomatal density and canopy temperature was evaluated in the model *C*<sub>4</sub> genus, *Setaria*. Recombinant inbred lines (RILs) derived from a *Setaria italica* × *Setaria viridis* cross were grown with ample or limiting water supply under field conditions in Illinois. An optical profilometer was used to rapidly assess stomatal patterning, and canopy temperature was measured using infrared imaging. Stomatal density and canopy temperature were positively correlated but both were negatively correlated with total above-ground biomass. These trait relationships suggest a likely interaction between stomatal density and the other drivers of water use such as stomatal size and aperture. Multiple quantitative trait loci (QTL) were identified for stomatal density and canopy temperature, including co-located QTL on chromosomes 5 and 9. The direction of the additive effect of these QTL on chromosome 5 and 9 was in accordance with the positive phenotypic relationship between these two traits. This, along with prior experiments, suggests a common genetic architecture between stomatal patterning and WUE in controlled environments with canopy transpiration and productivity in the field, while highlighting the potential of *Setaria* as a model to understand the physiology and genetics of WUE in *C*<sub>4</sub> species.**

**Keywords:** Canopy temperature, drought, optical tomography, quantitative trait loci, *Setaria*, stomata.

## Introduction

Drought stress is the primary limiting factor to crop production worldwide (Boyer, 1982). This is underpinned by the unavoidable loss of water vapor from leaves, via stomata, to the atmosphere in order for CO<sub>2</sub> to move in the reverse direction and be assimilated through photosynthesis. In the coming decades, crops are likely to experience increasingly erratic rainfall patterns, with more frequent and intense droughts, due to climate change (Stocker *et al.*, 2013). Irrigation of crops already accounts for ~70% of freshwater use, limiting the sustainability of any increase in irrigation to address drought limitations (Hamdy *et al.*, 2003). Consequently, there is great interest in understanding and improving crop water use efficiency (WUE; Leakey *et al.*, 2019) as well as crop drought resistance (Cattivelli *et al.*, 2008).

Substantial advances have been made in understanding WUE and drought resistance at the genetic, molecular, biochemical, and physiological levels in the model species, *Arabidopsis thaliana* (Zhang *et al.*, 2004; Valliyodan and Nguyen, 2006; Nakashima *et al.*, 2012). Unfortunately, efforts to translate this knowledge into improved performance of crop plants in the production environment have not resulted in success as frequently as hoped (e.g. Nelson *et al.*, 2007; Nemali *et al.*, 2015). Physiological, agronomic, and breeding studies directly in crops have also resulted in improved drought avoidance and drought tolerance (e.g. Condon *et al.*, 2004; Sinclair *et al.*, 2017), but there are challenges associated with trying to apply modern systems biology and bioengineering tools to crops that are relatively large in stature and have generation times of several months. Consequently, *Setaria viridis* (L.) has been proposed as a model C<sub>4</sub> grass that has characteristics that make it tractable for systems and synthetic biology while also being closely related to key C<sub>4</sub> crops, so that discoveries are more likely to translate to production crops (Brutnell *et al.*, 2010; Li and Brutnell, 2011). This study aimed to assess natural genetic variation in *Setaria* for two key traits related to WUE and drought response: stomatal density and canopy temperature (as a proxy for the rate of whole-plant water use).

*Setaria italica* and *S. viridis* are model C<sub>4</sub> grasses belonging to the panicoideae subfamily, which also includes maize, sorghum, sugarcane, miscanthus, and switchgrass (Brutnell *et al.*, 2010; Li and Brutnell, 2011). Foxtail millet (*S. italica*) is also a food crop in China and India (Devos *et al.*, 1998). The availability of sequence data for its relatively small diploid (2*n*=18) genome, short life cycle, small stature, high seed production, and amenability for transformation make *Setaria* a good model species for genetic engineering (Brutnell *et al.*, 2010; Bennetzen *et al.*, 2012). In addition, *Setaria* is adapted to arid conditions and is a potential source of genes conferring WUE and drought resistance.

Whole-plant WUE is the ratio of plant biomass accumulated to the amount of water used over the growing season (Condon *et al.*, 2004; Morison *et al.*, 2007; Blum, 2009; Tardieu, 2013). WUE at the leaf level is a complex trait controlled by factors

including photosynthetic metabolism, stomatal characteristics, mesophyll conductance, and hydraulics (Farquhar *et al.*, 1989; Condon *et al.*, 2002; Hetherington and Woodward, 2003). At the whole-plant scale, it is modified by canopy architecture, and root structure and function (Martre *et al.*, 2001; White and Snow, 2012).

Stomata regulate the exchange of water and carbon dioxide (CO<sub>2</sub>) between the internal leaf airspace and the atmosphere (Hetherington and Woodward, 2003; Bertolino *et al.*, 2019). Stomatal conductance (*g<sub>s</sub>*), which is the inverse of the resistance to CO<sub>2</sub> uptake and water loss, is controlled by a combination of stomatal density, patterning across the leaf surface, maximum pore size, and operating aperture (Faralli *et al.*, 2019; Nunes *et al.*, 2020). Of these traits, stomatal density is most simple to measure (Dow and Bergmann, 2014). Consequently, genetic variation in stomatal density has been explored in a range of species, including the identification of quantitative trait loci (QTL) in rice (Laza *et al.*, 2010), wheat (Schoppach *et al.*, 2016; Shahinnia *et al.*, 2016), barley (Liu *et al.*, 2017), *Arabidopsis* (Dittberner *et al.*, 2018; Delgado *et al.*, 2019), brassica (Hall *et al.*, 2005), poplar (Dillen *et al.*, 2008), and oak (Gailing *et al.*, 2008). However, there is a notable knowledge gap regarding genetic variation in stomatal density within C<sub>4</sub> species. While many genes involved in the regulation of stomatal development are known in *Arabidopsis*, investigation of whether their orthologs retain the same function in grasses and other phylogenetic groups that include the major crops is still relatively nascent (e.g. Raissig *et al.*, 2017; Lu *et al.*, 2019; Mohammed *et al.*, 2019). This is in part because standard protocols for measuring stomatal density are still laborious and time consuming, which slows the application of quantitative, forward, and reverse genetics approaches to identifying candidate genes and confirmation of their function. Therefore, improved methods for acquiring and analyzing images of stomatal guard cell complexes and other cell types in the epidermis are an area of active research (Haus *et al.*, 2015; Dittberner *et al.*, 2018; Fetter *et al.*, 2019; Li *et al.*, 2019). In addition, alternative approaches to rapidly screen stomatal conductance or rates of transpiration at the leaf and canopy scales (including temperature as a proxy) have also been developed and used to reveal genetic variation in traits related to drought stress and WUE (Liu *et al.*, 2011; Bennett *et al.*, 2012; Awika *et al.*, 2017; Prado *et al.*, 2018; Deery *et al.*, 2019; Vialet-Chabrand and Lawson, 2019). However, the links between genetic variation in stomatal density and measures of water use, which would be expected in theory, are rarely tested and, when tested, the results are inconsistent (e.g. Fischer *et al.*, 1998; Ohsumi *et al.*, 2007; Kholová *et al.*, 2010; Schoppach *et al.*, 2016).

To address these questions, we used a field study of a biparental mapping population developed from an interspecific cross between *S. viridis* (A10) and *S. italica* (B100).

The study was designed with the aim of (i) applying rapid, image-based methods for phenotyping stomatal density and

canopy water use; (ii) identifying variation in stomatal patterning, canopy temperature, and productivity; (iii) assessing trait relationships between stomatal density, canopy temperature, and biomass production; and (iv) identifying QTL for these traits in *Setaria*, grown in the field under wet and dry treatments.

## Materials and methods

### Plant material

This study used a population of 120 F<sub>7</sub> recombinant inbred lines (RILs), which were generated by an interspecific cross between domesticated *S. italica* accession B100 and a wild-type *S. viridis* accession A10 (Devos *et al.*, 1998; Wang *et al.*, 1998).

### Greenhouse experiment

Variation in stomatal density among the RILs was assessed in a greenhouse study at the University of Illinois, Urbana-Champaign in 2015. Plants were grown in pots (10×10×8.75 cm) filled with potting mixture (Metro-Mix 360 plus, Sun Gro Horticulture). Three seeds were sown directly into the pot. After germination, plants were thinned to one plant per pot. Growth conditions were 30/24 °C during the day/night and plants received supplemental photosynthetically active radiation from high-pressure sodium and metal halide lamps during the day (350 μmol m<sup>-2</sup> s<sup>-1</sup> on a 16 h day/8 h night cycle). Throughout the growing period, water was added to pot capacity along with fertilizer (EXCEL-CAL-MAG 15-5-5) 2–3 times a week.

The youngest fully expanded leaf was excised from the plant 17–22 days after sowing (DAS), covered in a wet paper towel, sealed in airtight bags, and stored at 4 °C. Within 48 h, a sample was excised with a razor blade from midway along the leaf to provide a cross-section from one leaf margin to the midrib (~20–30 mm length, 3–20 mm wide). This sample was attached to a glass microscope slide using double-sided adhesive tape, and the abaxial surface was immediately imaged using a μsurf explorer optical topometer (Nanofocus, Oberhausen, Germany; Haus *et al.*, 2015). Two fields of view in a transect from the midrib to the edge of a single leaf were imaged using a ×20 magnification objective lens with 0.6 numerical aperture. The instrument generates a grayscale image in the proprietary \*.nms format with dimensions of 0.8×0.8 mm in the *x*- and *y*-axes by stacking all the focused pixels across planes of the *z*-axis. The images were then exported into TIF files (Supplementary Fig. S1) and the stomatal number was manually counted using the cell counter tool in ImageJ software (<http://rsbweb.nih.gov/ij/>). Stomatal density was calculated by normalizing the number of stomata with the area of the field of view (0.64 mm<sup>2</sup>). Data from each of the four fields of view were treated as subsamples and averaged to estimate mean stomatal density for each replicate plant of a given RIL (Supplementary Table S1).

### Field experiment

The field experiment to assess variation in canopy temperature and total above-ground biomass was conducted at the SoyFACE field site, University of Illinois, Urbana-Champaign in 2015, in the manner described by Feldman *et al.* (2017). The average air temperature over the growing season was 21.5 °C with a relative humidity of 82% (Supplementary Fig. S2). In brief, plants were germinated in plug trays in the greenhouse and then, at 9 DAS, seedlings were hand transplanted (15 July 2015) into plots at the field site. Twelve retractable awnings (Gray *et al.*, 2016) were placed over the plots to block all water from any rainfall event in both wet and dry treatments (Supplementary Fig. S3). Drip

irrigation was supplied once a week in order to maintain greater soil moisture in the wet treatment.

Each genotype subplot in the experiment measured 25×20 cm and contained 30 plants with a grid spacing of 5 cm between the plants. There was a 25 cm space for the aisle between two columns of plots and 10 cm spacing between the rows of plots. Each awning contained 66 subplots including six check plots of the B100 accession. The volumetric water content in the center of each awning was measured every 15 min throughout the growing season using soil moisture probes (CS650; Campbell Scientific) at 5 cm and 25 cm depths.

Canopy temperature of all field plots under both wet and dry treatments was measured 30 and 32 DAS once canopy closure had occurred in all plots (Supplementary Table S2). A telescopic boom lift was used to collect images from a height of 9.1 m above the ground using a hand-held infrared camera (FLIR T400, FLIR Systems, Boston, MA, USA). On each date, one infrared and one RGB image was acquired for each awning, which consisted of 66 plots (Fig. 1). The time of the measurements was between 11.00 h and 15.00 h. Infrared imaging was performed only during clear and sunny weather conditions. Data from the 36 pixels at the center of each genotype subplot were used to estimate the canopy temperature (FLIR Tools, FLIR Systems). This ensured that temperature data were only sampled from pixels completely covered by plant canopy and not containing data from soil in the nearby aisles between plots. The data from the two dates were not structured in a way that would justify treating them as a repeated measure and therefore they were considered as two separate traits (CT-T1 and CT-T2).

Three plants from the center of each plot were destructively harvested 30 d after panicle emergence to estimate the shoot biomass (Supplementary Table S3). The plants were cut at the base, and the leaf, stem, and the panicles were separated and dried at 65 °C. The dried weights of leaf, stem, and panicle were summed to obtain the total shoot biomass. Culm height and tiller height were measured on the same plants from the base of the plant to the ligule of the youngest fully expanded leaf (Supplementary Table S4). Panicle emergence was measured as the number of days after sowing at which the panicle head was seen past the collar of the culm flag leaf in at least half of the individuals in a genotype-specific subplot (Supplementary Table S4).

### Data analysis

The greenhouse experiment was conducted with four replicates of each RIL arranged in a randomized complete block design with 120 genotypes as described in the equation below, where  $Y_{ij}$  is the individual observation of the trait of interest,  $\mu$  is the overall mean, Genotype<sub>*i*</sub> is the effect of the *i*th genotype, Block<sub>*j*</sub> is the effect of the *j*th block, and  $\epsilon_{ij}$  is the error term.

$$Y_{ij} = \mu + \text{Genotype}_i + \text{Block}_j + \epsilon_{ij}$$

The field experiment was conducted as a randomized complete block design in a split plot arrangement with three blocks, two treatment conditions, 12 awnings nested within treatments and blocks, and 120 genotypes as described below:

$$Y_{ijkl} = \mu + \text{Block}_i + \text{Treatment}_j + \epsilon_{ij} + \text{Awning}_{k(ij)} + \text{Genotype}_l + \text{Genotype} \times \text{Treatment}_{jl} + \epsilon_{ikl}$$

where  $Y_{ijkl}$  is the individual observation of the trait of interest,  $\mu$  is the overall mean, Block<sub>*i*</sub> is the effect of the *i*th block, Treatment<sub>*j*</sub> is the effect of the *j*th treatment,  $\epsilon_{ij}$  is the first error term, Awning<sub>*k(ij)*</sub> is the *k*th awning nested within Block<sub>*i*</sub> and Treatment<sub>*j*</sub>, Genotype<sub>*l*</sub> is the *l*th genotype, Genotype×Treatment<sub>*jl*</sub> is the interaction between Genotype<sub>*l*</sub> and Treatment<sub>*j*</sub>, and  $\epsilon_{ikl}$  is the second error term.

The broad sense heritability was computed using the variance components from the mixed model using the formula below.

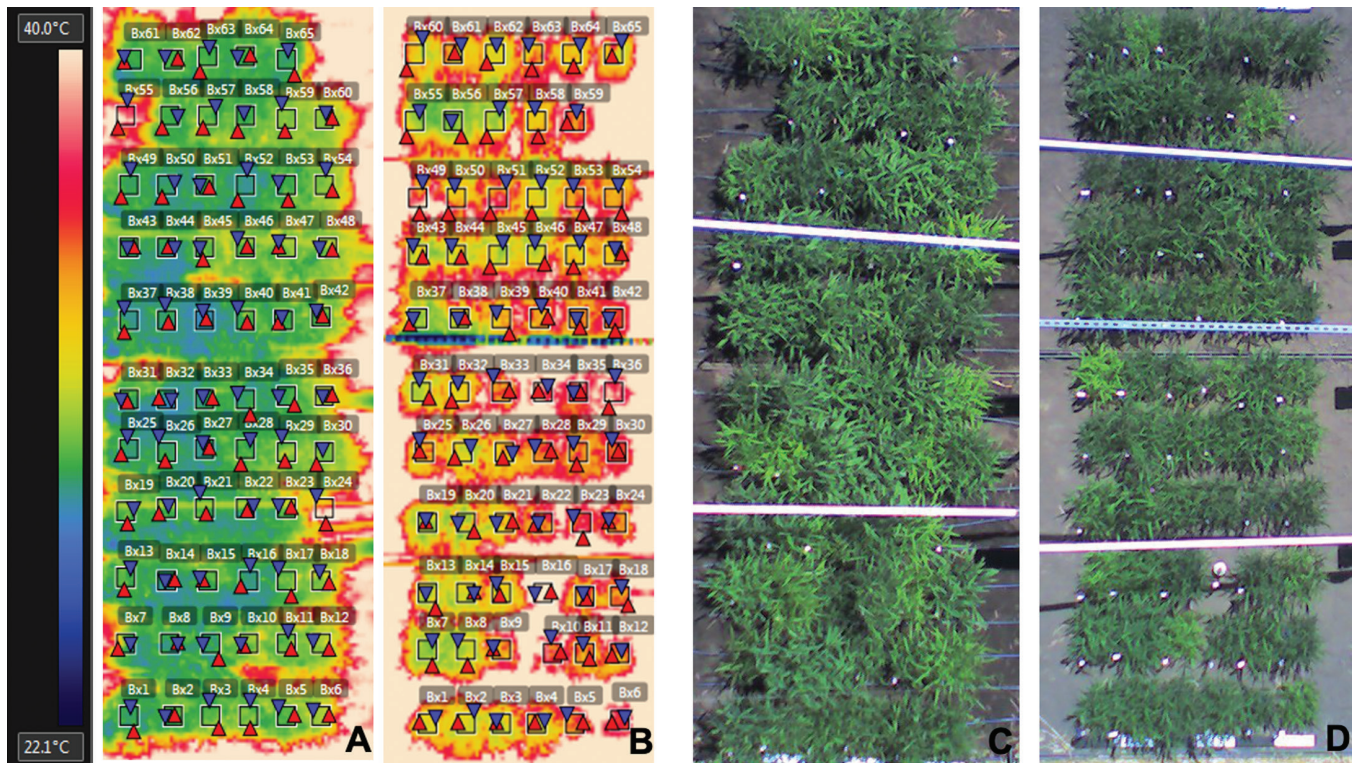


**Fig. 1.** Aerial infrared and RGB images of *Setaria* subplots under awnings in wet and dry treatments. Infrared image of wet awning (A) and dry awning (B). RGB image of wet awning (C) and dry awning (D). The square boxes are the measured area of each subplot canopy.

$$H_{\text{broad sense}}^2 = \frac{\sigma_{(\text{Genotype})}^2}{\sigma_{(\text{Genotype})}^2 + \frac{\sigma_{(\text{Genotype} \times \text{Treatment})}^2}{n_{\text{treatments}}} + \frac{\sigma_{(\text{residual})}^2}{n_{\text{reps}}}}$$

The variance components from the mixed model were extracted using the lme4 package in R (Bates *et al.*, 2015). Best linear unbiased predictors (BLUPs) were calculated for each trait of interest using the experimental designs discussed earlier where genotypes and blocks were considered as random effects and treatment and awning as fixed effects. Phenotypic correlations were computed using the ggplot2 package (Wickham, 2016) in R software to determine the strength and directionality of the relationship between all the traits collected in this study.

The QTL mapping was performed on the BLUP values for stomatal density and canopy temperature under different treatments and sampling dates using ~1400 single nucleotide polymorphism (SNP) markers. Mapping was performed using a custom biparental linkage mapping program (Feldman *et al.*, 2017) based upon the functionality encoded within the R/qlt (Broman *et al.*, 2003) and funql (Kwak *et al.*, 2014) packages in R. All codes used can be found at [https://github.com/maxfeldman/foxy\\_qtl\\_pipeline](https://github.com/maxfeldman/foxy_qtl_pipeline). A two-step procedure was performed (Feldman *et al.*, 2017). First, a single QTL model genome scan was performed using Haley–Knott regression to identify QTL with a logarithm of odds (LOD) score higher than the significant threshold obtained through 1000 permutations at alpha 0.05. Second, a stepwise forward/backward selection procedure was performed to identify an additive, multiple QTL model based upon maximization of the penalized LOD score. The two-step procedure was conducted on all the traits and time points. QTL that lie within a 20 cM window were considered to be co-located (Feldman *et al.*, 2017).

## Results

### Soil moisture profile

Soil moisture content was equivalent in the wet and dry treatments at the beginning of the experiment (Fig. 2). As time progressed, plants in the wet treatment continued to have adequate water supply (30–40% v/v) throughout the growing period. In contrast, plants in the dry treatment experienced progressively drier soil conditions as the water they transpired was not replaced by rainfall or irrigation. The soil moisture was reduced in the dry treatment compared with the wet treatment at 5 cm and 25 cm depth by 20 DAS, resulting in a statistically significant interaction between treatment and time ( $P < 0.001$ ) as well as significant overall effects of drought treatment ( $P < 0.001$ ), depth ( $P < 0.001$ ), and time ( $P < 0.001$ ). Midday canopy temperature data were collected after this date, 30 and 32 DAS, when plants in the dry treatment were experiencing rapidly decreasing availability of soil moisture. This indicates that while plants in the dry treatment were subjected to limited water supply, they were still physiologically active; that is, drought stress was moderate.

### Genotypic variation in stomatal density and canopy temperature

Among the 120 RILs, stomatal density on the abaxial surface of the youngest fully expanded leaf ranged between 58 and

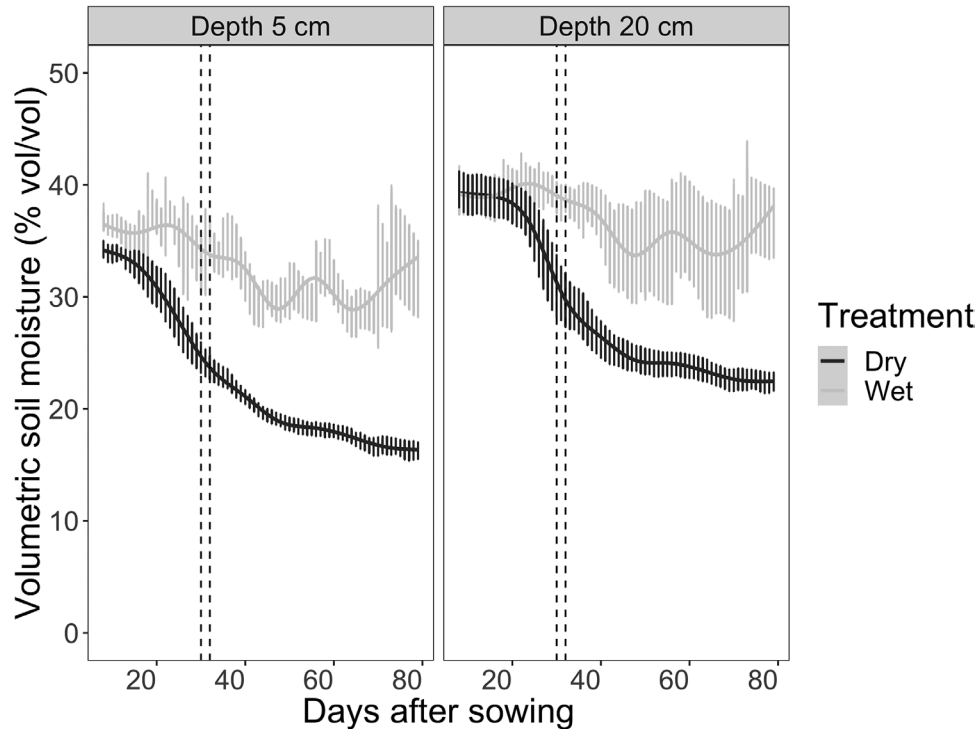


**Fig. 2.** Soil volumetric water content (% v/v) at depths of 5 cm and 25 cm over the growing season in plots of *Setaria* supplied with either regular irrigation to maintain adequate water supply (wet treatment; light gray) or receiving no irrigation (dry treatment; dark gray). Rainfall was blocked from entering plots of both treatments using retractable rainout shelters. Data points and error bars shown the mean and SE of three replicates per treatment. The dashed vertical lines indicate the dates when canopy temperature was measured.

115 stomata  $\text{mm}^{-2}$ , with a mean of 84 stomata  $\text{mm}^{-2}$  (Fig. 3; Supplementary Fig. S4). The broad sense heritability of stomatal density was 0.58. Among the 120 RILs, the mean canopy temperature at midday ranged from 28.8 °C to 31.9 °C at 30 DAS and from 28.6 °C to 31.9 °C at 32 DAS in the wet treatment, and from 30.9 °C to 39.2 °C at 30 DAS and from 29.3 °C to 38.1 °C at 32 DAS in the dry treatment. The mean midday canopy temperature across the RIL population was greater in the dry treatment than in the wet treatment at both 30 DAS (32.9 °C versus 29.9 °C;  $P < 0.001$ ) and 32 DAS (32.0 °C versus 29.6 °C;  $P < 0.001$ ; Fig. 4), with the treatment effect being slightly greater at 30 DAS (3.0 °C) than at 32 DAS (2.4 °C). Midday canopy temperature was positively correlated between the two measurement dates for both wet ( $\rho = 0.78$ ,  $P < 0.001$ ) and dry ( $\rho = 0.66$ ,  $P < 0.001$ ) conditions, which gives confidence in the phenotyping method (Supplementary Fig. S5). The broad sense heritability of canopy temperature was 0.54 and 0.40 at 30 and 32 DAS, respectively.

#### Phenotypic relationships among canopy temperature, stomatal density, and total biomass

Midday canopy temperature was negatively correlated with total above-ground biomass under both wet and dry treatments at both 30 DAS (wet:  $\rho = -0.38$ ,  $P < 0.001$ ; dry:  $\rho = -0.32$ ,  $P < 0.001$ ; Fig. 5A) and 32 DAS (wet:  $\rho = -0.49$ ,  $P < 0.001$ ; dry:  $\rho = -0.46$ ,  $P < 0.001$ ; Fig. 5B). The average

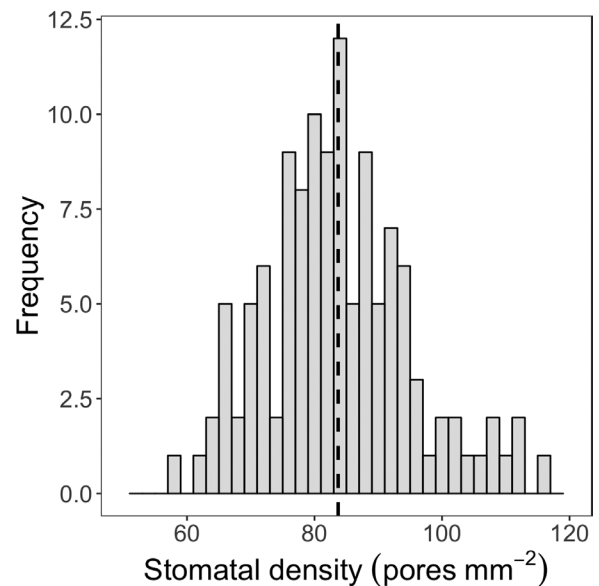


**Fig. 3.** Frequency distribution of stomatal density (pores  $\text{mm}^{-2}$ ) of 120 recombinant inbred lines derived from a cross of *S. italica* and *S. viridis*, and the B100 parental line. Data are genotype means derived from two fields of view per leaf from each of four replicate plants. The dotted vertical lines represent the population mean value.

increase in total above-ground biomass production associated with a decrease in midday canopy temperature of 1 °C was greater in the wet treatment than in the dry treatment

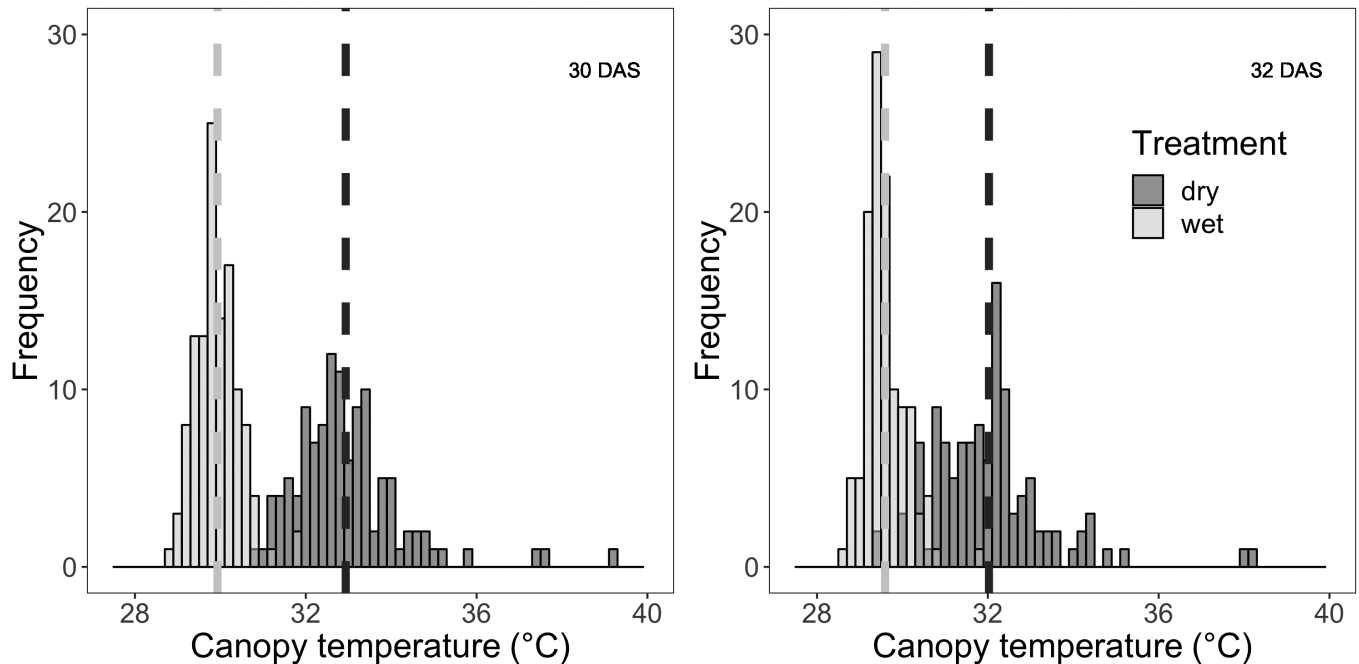


**Fig. 4.** Frequency distribution of canopy temperature ( $^{\circ}\text{C}$ ) of 120 RILs in wet (light gray) and dry (dark gray) treatments at 30 and 32 days after sowing (DAS). Data are means derived from all pixels in the interior of three replicate plots per genotype. The dashed vertical lines represent the treatment mean value for each treatment.

on both measurement dates (Table 1). The amount of variation in total above-ground biomass production explained by variation in midday canopy temperature was slightly greater in the wet treatment than in the dry treatment on both sampling dates (Table 1). The parental line A10 was one of the genotypes with the lowest biomass and highest canopy temperature under both treatments and days of measurement, while the parental line B100 had trait values that were close to the mean of the population.

Stomatal density was positively correlated with midday canopy temperature under both wet and dry treatments at both 30 DAS (wet:  $\rho=0.40$ ,  $P<0.001$ ; dry:  $\rho=0.38$ ,  $P<0.001$ ; Fig. 5C) and 32 DAS (wet:  $\rho=0.37$ ,  $P<0.001$ ; dry:  $\rho=0.39$ ,  $P\leq 0.001$ ; Fig. 5D). Correspondingly, stomatal density was negatively correlated with total above-ground biomass under both dry ( $\rho=-0.33$ ,  $P\leq 0.001$ ) and wet ( $\rho=-0.23$ ,  $P=0.012$ ) conditions (Fig. 6). The correlation between stomatal density and total biomass was stronger under the dry treatment than under the wet treatment. Stomatal density was not significantly correlated with panicle emergence date, tiller height, or culm height in either wet or dry treatments (Supplementary Figs S6, S7).

#### QTL mapping results

QTL analysis identified a total of 32 QTL across seven traits, including three significant loci for stomatal density and eight significant loci for canopy temperature (Table 2; Fig. 7). The proportion of phenotypic variation associated with these QTL ranged between 8% and 23% for both stomatal density and

canopy temperature. On chromosome 9 at  $\sim 40$  cM, a QTL for stomatal density co-located with QTL for canopy temperature, biomass production, and culm height under both wet and dry treatments (Fig. 7). The effect of the B100 allele was negative for stomatal density and canopy temperature while being positive for biomass and culm height (Fig. 7). On chromosome 5, a QTL for stomatal density co-located with QTL for canopy temperature, culm height, and tiller height. The effect of the B100 allele at this location was negative for all traits (Fig. 7). The QTL for the date of panicle emergence overlapped with the QTL for canopy temperature on chromosome 7, with consistent allelic effects across all trait and treatment combinations (Fig. 7).

#### Discussion

This study successfully characterized phenotypic and genetic variation in stomatal density, rates of canopy water use, and productivity in *Setaria*, which can be used as a foundation for future studies to apply systems biology approaches to advance understanding of WUE and drought resistance in  $C_4$  species. Significant trait correlations were detected among stomatal density, canopy temperature, and total above-ground biomass in both the wet and dry treatments.

The stomatal densities of RILs in this population ( $58\text{--}115\text{ mm}^{-2}$ ; Fig. 3) were slightly greater than previously reported for faba bean ( $30\text{--}75\text{ mm}^{-2}$ , Khazaei *et al.*, 2014) and wheat ( $36\text{--}92\text{ mm}^{-2}$ , Schoppach *et al.*, 2016;  $43\text{--}92\text{ mm}^{-2}$ , Shahinnia

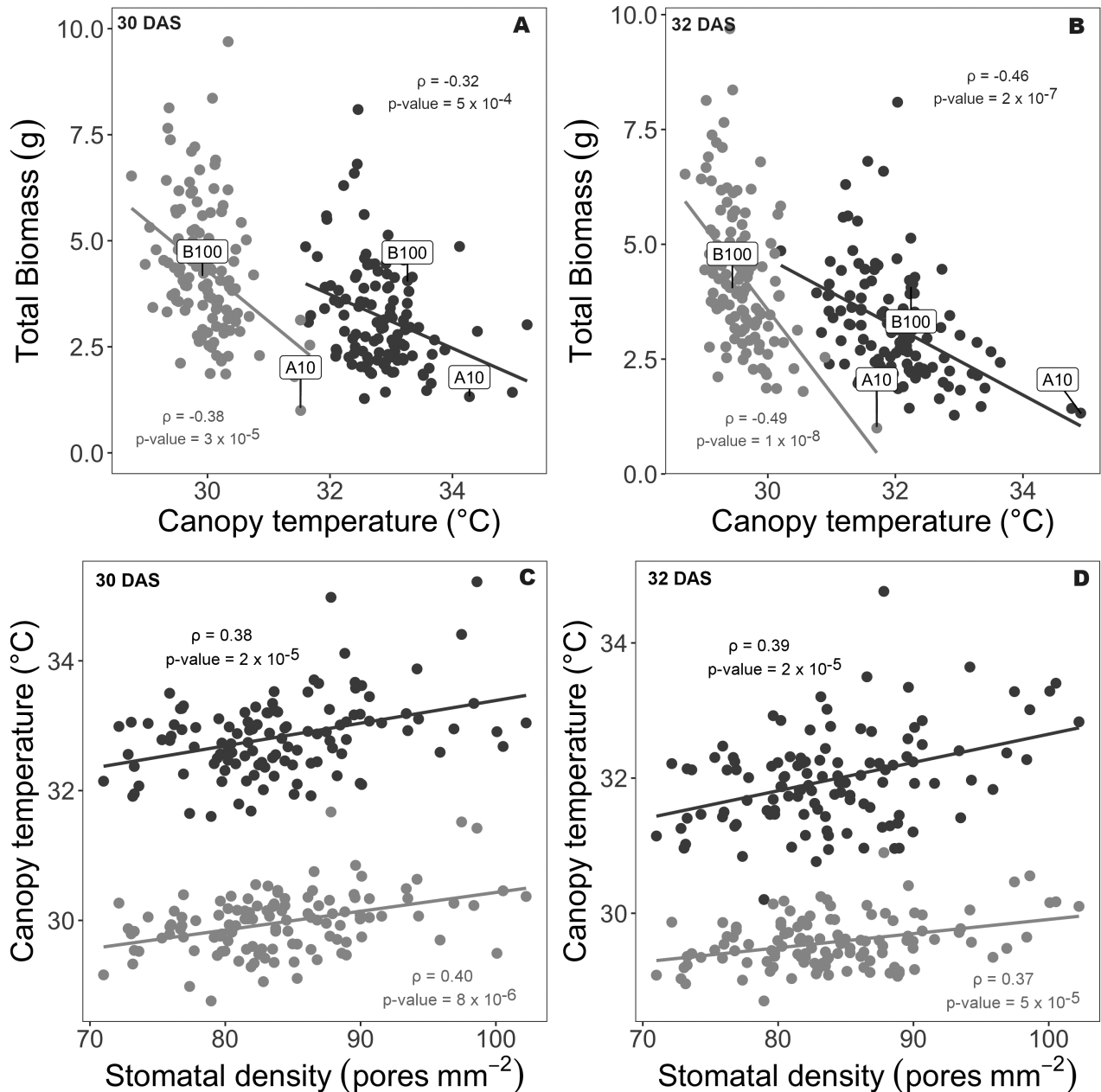


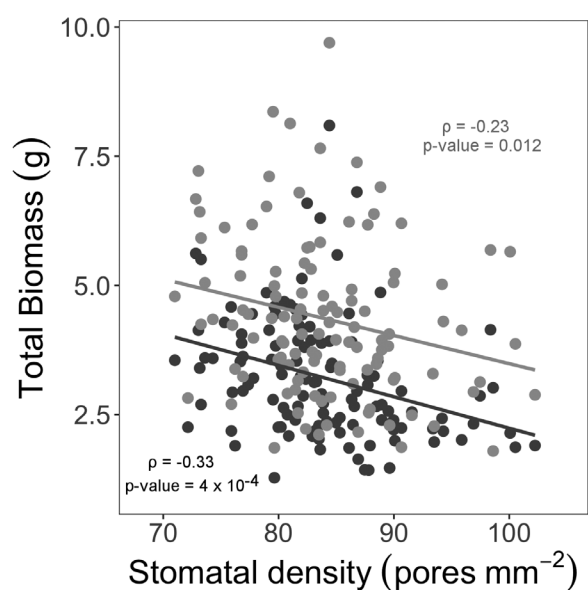
**Fig. 5.** (A and B) Scatterplot of total biomass (g per plant) in relation to canopy temperature (°C) for *Setaria* RILs and the parent lines (A10 and B100) under wet (gray circles) and dry conditions (black circles) at 30 and 32 days after sowing (DAS). (C and D) Scatterplot of canopy temperature (°C) in relation to stomatal density (pores  $\text{mm}^{-2}$ ) for *Setaria* RILs and the parent lines (A10 and B100) under wet (gray) and dry (black) conditions at 30 and 32 DAS. Data are best linear unbiased predicted (BLUP) values for each genotype. Lines of best fit are shown along with the Pearson's correlation coefficient ( $\rho$ ) and associated  $P$ -value.

*et al.*, 2016), but generally lower than for *Arabidopsis* (90–210  $\text{mm}^{-2}$  Dittberner *et al.*, 2018) and rice (273–697  $\text{mm}^{-2}$ , Laza *et al.*, 2010; 200–400  $\text{mm}^{-2}$ , Kulya *et al.*, 2018). While the magnitude of variation in stomatal density among the RIL population was sufficient to allow for QTL mapping and analysis of trait correlations, the parents of the population were not selected on the basis of this trait. Thus, the resulting magnitude of variation across the population was relatively modest.

It would be valuable to investigate how much more variation for stomatal density may be found among genotypes within either *S. italica* or *S. viridis*, as well as the genus as a whole. The present study provided a proof of concept for the use of optical tomography to image the leaf epidermis. As proposed by Haus *et al.* (2015), optical tomography does not require sample preparation steps and can also be used on frozen leaf samples. This was significantly less laborious and more convenient than

**Table 1.** Regression parameters for total above-ground biomass (g per plant) in relation to canopy temperature (°C) and stomatal density (pores per mm<sup>2</sup>) of *Setaria* genotypes grown under wet and dry treatments

			Intercept (b)	Slope (a)	R <sup>2</sup>	P-value
Biomass=Intercept (b)+a (Canopy temperature)						
Canopy temperature	30 DAS	Wet	40.00	-1.19	0.13	<0.001
		Dry	24.02	-0.63	0.09	<0.001
	32 DAS	Wet	58.21	-1.82	0.24	<0.001
		Dry	27.01	-0.74	0.20	<0.001
Biomass=Intercept (b)+a (Stomatal density)						
Stomatal density	Wet		8.94	-0.05	0.05	0.012
	Dry		8.31	-0.06	0.10	<0.001

**Fig. 6.** Scatterplot of total biomass (g per plant) relative to stomatal density (pores mm<sup>-2</sup>) for *Setaria* RILs and the parent lines (A10 and B100) under wet (gray) and dry (black) conditions. Data are best linear unbiased predicted (BLUP) values for each genotype. Lines of best fit are shown along with the Pearson's correlation coefficient ( $\rho$ ) and associated  $P$ -value.

standard methods of taking leaf imprints of fresh leaves with dental gum and nail varnish (Rowland-Bamford *et al.*, 1990).

The magnitude of variation in canopy temperature across the *Setaria* RIL population was similar to that observed for sorghum (Awika *et al.*, 2017) and wheat (Mason *et al.*, 2013) RIL populations. Variations in canopy temperature among the RIL population were similar on 30 DAS (wet 3.1 °C, dry 8.3 °C; Fig. 4) and 32 DAS (wet 3.3 °C, dry 8.8 °C; Fig. 4), and canopy temperature was correlated across the two dates sampled for both the wet ( $r=0.78$ ) and dry treatments ( $r=0.66$ ) (Supplementary Fig. S5). This might be considered surprising given the highly dynamic nature of canopy temperature in response to wind gusts, diurnal variation in solar radiation, and daily or seasonal variation in climate. However, the reproducibility of the data across dates is consistent with the comprehensive analysis by Deery *et al.* (2019), which analyzed 98 independent time points of canopy temperature data collected

for a wheat population over 14 dates in 2 years. These authors concluded that canopy temperature could be reliably screened from one or two sampling points if data were collected under clear sky conditions in the afternoon, as was done in the current study. The present study also highlighted *Setaria* as a highly tractable model for field trials because its small stature allows non-destructive, remote-sensing approaches to phenotyping, such as thermal imaging, to be performed on hundreds of replicated plots using hand-held cameras and a boom lift. This is significantly simpler in terms of data acquisition and data analysis than using drones or vehicles to gather data across field trials of crops with larger stature that require field trials covering larger areas (Deery *et al.*, 2016; Sagan *et al.*, 2019).

Canopy temperature was negatively correlated with the total above-ground biomass of the *Setaria* RILs under both wet and dry conditions (Fig. 5A, B). This is consistent with RILs that had higher temperatures due to less evaporative cooling being able to assimilate less CO<sub>2</sub>, and therefore producing less biomass, which was expected based on theory and previous studies (Fischer *et al.*, 1998; Jones, 2004). In addition, canopy temperature was significantly greater in the dry treatment compared with the wet treatment (Fig. 5A, B), which was consistent with stomatal closure reducing water use and evaporative cooling when there is limited water availability (Turner *et al.*, 2001). The relationship between canopy temperature and biomass was stronger in the wet treatment than in the dry treatment on both measurement dates (Fig. 5A, B). This was reflected in canopy temperature explaining a greater proportion of variation in biomass (i.e. greater correlation coefficient) and a greater loss of biomass production per unit increase in canopy temperature under wet than under dry conditions (Fig. 5A, B). This pattern of response is also consistent with prior observations (Bennett *et al.*, 2012; Mason *et al.*, 2013), but does not appear to have been the subject of much discussion. While it may seem initially counterintuitive that the relationship between the rate of water use and productivity would be weaker when water is limiting, it is consistent with genotypes that have inherently high rates of transpiration (i.e. cooler canopies) having greater reductions in productivity in response to drought stress than genotypes with inherently low rates of transpiration (i.e. warmer canopies). We suggest that this differential response may be



**Table 2.** Putative quantitative trait loci (QTL) for stomatal density (SD), canopy temperature at 30 DAS (CT-T1) and 32 DAS (CT-T2), biomass (BM), culm height (CH), panicle emergence (PE), and tiller height (TH) traits in the 120 F<sub>7</sub> recombinant inbred line population derived from a cross of *S. italica* and *S. viridis*, and the B100 parental line

Trait	Treat- ment	Peak marker	Chr	Pos (cM) <sup>a</sup>	LOD at peak <sup>b</sup>	Variance (%) <sup>c</sup>	Additive effect	Left CI (cM) <sup>d</sup>	Right CI (cM)
BM	Dry	S2_37761700	2	69.7	5.0	12.6	-1.8	69.2	70.0
	Dry	S2_37820883	2	70.0	6.9	17.9	2.1	69.7	71.1
	Dry	S9_6724364	9	34.9	5.4	13.5	0.4	30.6	38.6
	Wet	S1_31298551	1	66.9	2.5	5.4	0.2	61.1	83.0
	Wet	S2_37761700	2	69.7	4.8	10.8	-1.7	69.2	70.0
	Wet	S2_37820883	2	70.0	6.9	16.2	2.1	69.7	71.1
	Wet	S9_6724364	9	34.9	6.3	14.7	0.4	31.3	38.6
CH	Dry	S5_41999990	5	100.4	7.5	20.5	-50.6	97.7	101.1
	Dry	S9_5686516	9	32.0	5.4	14.2	41.8	29.4	36.4
	Wet	S1_35287681	1	80.1	7.1	8.0	36.5	78.3	83.5
	Wet	S2_26339986	2	43.7	4.2	4.4	37.1	39.9	44.9
	Wet	S2_37820883	2	70.0	3.4	3.6	28.5	59.6	75.4
	Wet	S3_2542615	3	16.5	6.6	7.3	35.2	11.4	20.7
	Wet	S5_41999990	5	100.4	19.4	28.4	-76.5	100.2	100.7
CT-T1	Wet	S9_6724364	9	34.9	9.5	11.3	45.8	32.8	36.4
	Dry	S5_39309008	5	93.8	5.7	14.1	-0.2	92.8	100.2
	Dry	S7_32133319	7	99.9	8.0	21.1	0.4	92.5	101.9
	Dry	S9_7218054	9	35.9	6.0	15.0	-0.2	32.8	38.6
	Wet	S5_39309008	5	93.8	4.4	10.0	-0.2	76.2	104.1
	Wet	S7_31494503	7	93.3	9.2	23.1	0.3	89.3	101.9
	Wet	S9_6724364	9	34.9	8.8	21.8	-0.2	33.9	38.6
CT-T2	Wet	S7_31494503	7	93.3	3.8	12.0	0.2	89.3	101.9
	Wet	S9_6724364	9	34.9	6.4	21.0	-0.2	32.8	38.6
PE	Dry	S7_31178325	7	89.3	6.7	21.5	1.8	85.8	101.9
	Dry	S9_54618932	9	164.4	3.3	10.1	1.1	140.7	168.5
	Wet	S2_43563669	2	90.6	3.8	9.5	1.1	69.7	95.7
	Wet	S7_32133319	7	99.9	8.5	23.3	2.2	93.3	101.9
SD	Wet	S9_54618932	9	164.4	4.8	12.2	1.2	160.2	168.5
	Wet	S5_42996052	5	104.8	8.3	20.8	-3.8	101.1	106.6
	Wet	S9_10073675	9	45.6	5.0	11.6	-2.3	40.4	52.7
TH	Wet	S9_50690449	9	136.5	3.7	8.3	-2.0	133.0	146.9
	Wet	S5_42757204	5	104.4	9.8	33.7	-62.8	99.2	106.1

<sup>a</sup> Position of the peak marker in centiMorgans (cM).<sup>b</sup> Logarithm of odds (LOD) of the peak marker.<sup>c</sup> Percentage of phenotypic variance explained by the QTL.<sup>d</sup> Left confidence interval of the QTL.

conserved. Also, it adds weight to the argument that genetic variation in WUE is best screened under well-watered conditions (Leakey *et al.*, 2019).

The positive correlation of stomatal density with the canopy temperature under drought stress suggests that the relationship between these two traits is complicated (Fig. 5C,D), since—if all else is equal—greater stomatal density would be expected to increase transpiration and lead to canopy cooling (Dow and Bergmann, 2014). Consistent with that theory, previous studies have reported that stomatal density is positively correlated with WUE (Xu and Zhou, 2008). However stomatal conductance is influenced by multiple factors, including stomatal density, maximum size, and operating aperture (Dow and Bergmann, 2014; Faralli *et al.*, 2019). In addition, there are

multiple examples across diverse species where the expected positive correlation between stomatal density and stomatal conductance was not observed (Jones, 1977; Liao *et al.*, 2005; Ohsumi *et al.*, 2007). So, it is plausible that greater stomatal density within this population of *Setaria* RILs was associated with a developmental or functional shift that led to smaller stomatal apertures and lower rates of transpiration. As a result, within this population, lower stomatal density was also associated with greater biomass production. However, it should be noted that this relationship may be a function of the forced recombination across many parental alleles that is found in a RIL population. Breaking up gene linkage that can result from selection has been proposed to be a powerful approach to understand the biophysical basis for phenotypic relationships

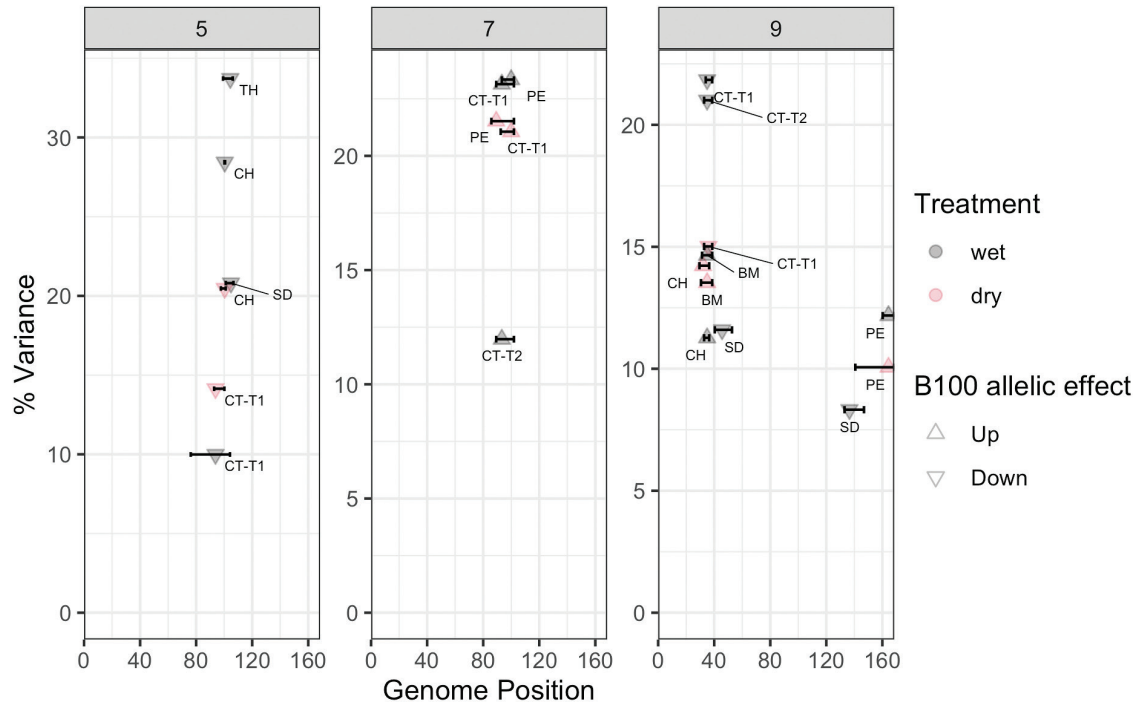


**Fig. 7.** QTL identified for stomatal density (SD) and canopy temperature at 30 DAS (CT-T1) and 32 DAS (CT-T2), total biomass (BM), panicle emergence (PE), culm height (CH), and tiller height (TH) under wet (gray) and dry (pink) treatments in the *Setaria* RIL population. Each panel corresponds to a chromosome. The arrows indicate the direction of the B100 allelic effect.

(Des Marais *et al.*, 2013). The observed positive correlation may reflect the developmental trade-off where stomatal size and stomatal density are widely found to be negatively correlated due to a limited amount of space on the epidermis (Shahinnia *et al.*, 2016; Faralli *et al.*, 2019), but this needs to be confirmed experimentally. In contrast, stomatal density was either not correlated or was weakly, positively correlated with yield in wheat grown under both well-watered and drought treatments (Khazaie *et al.*, 2011; Schoppach *et al.*, 2016; Shahinnia *et al.*, 2016; Faralli *et al.*, 2019). So, the balance of trade-offs between stomatal density and aperture may be different among different biparental mapping populations, if not more generally in *Setaria* versus wheat. It would be valuable to compare if the same phenotypic relationship is observed across other biparental populations within these species as well as across natural accessions of these crops. New machine learning-enabled phenotyping methods for measuring stomatal size (e.g. Xie *et al.*, 2020, Preprint) will aid this effort, because manual estimation of stomatal size currently takes ~30 times longer than manually measuring stomatal density, making it infeasible to assess in many experiments.

This study identified three unique QTL each for stomatal density and canopy temperature (Fig. 7). All three of the canopy temperature QTL were robust in terms of being observed in both the wet and dry treatments. In addition, the canopy temperature QTL on chromosomes 5 and 9 co-localized with QTL for stomatal density (Fig. 7). Genetic fine mapping would be required to discount the possibility that there are two loci

in linkage at those locations, as <10% of the lines are discordant between the identified SNPs in each case. However, the observed pattern could be the result of pleiotropy, where a single locus regulates both traits. Additionally, this would be concordant with the consistent direction of the allelic effects and the positive correlation between stomatal density and temperature, as well as the theoretical expectation that stomatal patterning on the epidermis influences transpiration rates. It is notable that the allelic effects of the QTL identified for biomass production and culm height at ~40 cM on chromosome 9 are also consistent with the phenotypic correlations among the traits (Table 2). This opens up the possibility of pleiotropic effects at that locus across multiple measures of plant carbon and water relations which are logically linked to stomatal function.

Flowering time genes can have pleiotropic effects on stomatal apertures and stomatal conductance in *Arabidopsis* (Ando *et al.*, 2013; Kimura *et al.*, 2015; Auge *et al.*, 2019), but data were not reported in those studies on stomatal patterning. Flowering time in wheat also impacts WUE in a complex manner that is environmentally dependent (Condon *et al.*, 2004). Overlapping QTL for the date of panicle emergence and either stomatal density (chromosome 9) or canopy temperature (chromosome 7) opens up the possibility that similar processes occur in *Setaria*. However, the underlying basis of these interactions is not easily interpreted from the current data.

The ability to detect the same QTL in a greenhouse screen of stomatal density as for canopy temperature in the



above-ground productivity. Also, the effect of the B100 allele at each locus on canopy temperature was logically consistent with lower water use being associated with greater WUE, as measured gravimetrically on an indoor high-throughput phenotyping facility. This adds further evidence for the notion that controlled-environment and field studies of *Setaria* can be used in conjunction with one another when studying these traits. It is noteworthy that on chromosome 7 and at ~40 cM on chromosome 9, the percentage of the phenotypic variance explained by these QTL for stomatal density and canopy temperature, along with WUE, was generally greater than, or equal to, that for the other traits assessed to date. One explanation for this would be that these loci directly regulate traits related to stomatal function and then indirectly influence the other traits via effects on crop water use. There is no reason to think the experimental design used here results in any greater statistical power to detect genotype–phenotype associations than the other studies. However, additional experimentation where all traits are measured simultaneously is needed to test this notion definitively.

In conclusion, this study identified genetic loci in *Setaria* that are associated with variation in stomatal density as well as other traits important to WUE, productivity, and drought resistance. This suggests that *Setaria* is an experimentally tractable model system that would be highly suitable for more in-depth investigation of the mechanisms underpinning stomatal development and their influence on WUE in  $C_4$  species. An additional benefit to identifying QTL and genes in *Setaria* is that it is also an agronomic crop, so the findings could have direct relevance to crop improvement programs as well as potentially translating into benefits for close relatives including maize, sorghum, and sugarcane.

## Supplementary data

The following supplementary data are available at [JXB online](#).

Fig. S1. Representative images from optical tomography of abaxial leaf surfaces of *Setaria viridis* (A10) and *Setaria italica*.

Fig. S2. Daily average values of air temperature and relative humidity at the SoyFACE experimental field site

Fig. S3. Field experiment layout for canopy temperature and biomass measurements.

Fig. S4. Stomatal density of 120 recombinant inbred lines derived from a cross of *S. italica* and *S. viridis*, and the B100 parental line.

Fig. S5. Scatterplot of midday canopy temperature for *Setaria* RILs and B100 on 30 DAS versus 32 DAS under wet and dry treatments.

Fig. S6. Phenotypic trait correlations of stomatal density versus canopy temperature at 30 DAS (CT-T1) and 32 DAS (CT-T2), total biomass, panicle emergence, culm height, and tiller height under wet treatment conditions in this study.

Fig. S7. Phenotypic trait correlations of stomatal density versus canopy temperature at 30 DAS (CT-T1) and 32 DAS (CT-T2), total biomass, panicle emergence, culm height, and tiller height under dry treatment conditions in this study.

Table S1. Stomatal density per field of view of *setaria* abaxial leaf surface.

Table S2. Plot mean values for canopy temperature.

Table S3. Plot mean values for above-ground biomass.

Table S4. Plot mean values for tiller height, culm height and panicle emergence date.

## Acknowledgements

Funded by the U.S. Department of Energy under Prime Agreement nos DE-SC0008769 and DE-SC0018277. We thank Dr Timothy Werten for helping with the stomatal density sample collection, and other undergraduates and summer interns for their help with field management. We also thank many project partners from the Danforth Plant Science Center, Carnegie Institute, Washington State University, and University of Minnesota that helped with transplanting seedlings.

## Author contributions

ADBL and IB: conceptualization; ADB, PTP, DB, and REP: supervision; PTP: collection and processing of the thermal images; DX: collection of the stomatal images; PTP, DB, REP, and LF: management of the experiment and collection of biomass data; PTP, MF, IB, and ADBL: analysis and interpretation of the data; PTP and ADBL: writing; MF, IB, DB, REP, and LF: reviewing and commenting on the article.

## Data availability

Raw data are available as supplementary tables, and all images are available via the Dryad Digital Repository: <https://doi.org/10.5061/dryad.crjdfn33z> (Prakash *et al.*, 2021).

## References

- Ando E, Ohnishi M, Wang Y, Matsushita T, Watanabe A, Hayashi Y, Fujii M, Ma JF, Inoue S, Kinoshita T. 2013. TWIN SISTER OF FT, GIGANTEA, and CONSTANS have a positive but indirect effect on blue light-induced stomatal opening in Arabidopsis. *Plant Physiology* **162**, 1529–1538.
- Auge GA, Penfield S, Donohue K. 2019. Pleiotropy in developmental regulation by flowering-pathway genes: is it an evolutionary constraint? *New Phytologist* **224**, 55–70.
- Awika H, Hays D, Mullet J, Rooney W, Weers B. 2017. QTL mapping and loci dissection for leaf epicuticular wax load and canopy temperature depression and their association with QTL for staygreen in *Sorghum bicolor* under stress. *Euphytica* **213**, 207.
- Banan D, Paul RE, Feldman MJ, Holmes MW, Schlake H, Baxter I, Jiang H, Leakey ADB. 2018. High-fidelity detection of crop biomass quantitative trait loci from low-cost imaging in the field. *Plant Direct* **2**, e00041.
- Bates D, Maechler M, Bolker B, Walker S. 2015. Fitting linear mixed-effects models using lme4. *Journal of Statistical Software* **67**, 1–48.

- Bennett D, Reynolds M, Mullan D, Izanloo A, Kuchel H, Langridge P, Schnurbusch T.** 2012. Detection of two major grain yield QTL in bread wheat (*Triticum aestivum* L.) under heat, drought and high yield potential environments. *Theoretical and Applied Genetics* **125**, 1473–1485.
- Bennetzen JL, Schmutz J, Wang H, et al.** 2012. Reference genome sequence of the model plant *Setaria*. *Nature Biotechnology* **30**, 555–561.
- Bertolino LT, Caine RS, Gray JE.** 2019. Impact of stomatal density and morphology on water-use efficiency in a changing world. *Frontiers in Plant Science* **10**, 225.
- Blum A.** 2009. Effective use of water (EUW) and not water-use efficiency (WUE) is the target of crop yield improvement under drought stress. *Field Crops Research* **112**, 119–123.
- Boyer JS.** 1982. Plant productivity and environment. *Science* **218**, 443–448.
- Broman KW, Wu H, Sen S, Churchill GA.** 2003. R/qtl: QTL mapping in experimental crosses. *Bioinformatics* **19**, 889–890.
- Brutnell TP, Wang L, Swartwood K, Goldschmidt A, Jackson D, Zhu XG, Kellogg E, Van Eck J.** 2010. *Setaria viridis*: a model for C<sub>4</sub> photosynthesis. *The Plant Cell* **22**, 2537–2544.
- Casson SA, Hetherington AM.** 2010. Environmental regulation of stomatal development. *Current Opinion in Plant Biology* **13**, 90–95.
- Cattivelli L, Rizza F, Badeck F-W, Mazzucotelli E, Mastrangelo AM, Francia E, Marè C, Tondelli A, Stanca AM.** 2008. Drought tolerance improvement in crop plants: an integrated view from breeding to genomics. *Field Crops Research* **105**, 1–14.
- Condon AG, Richards RA, Rebetzke GJ, Farquhar GD.** 2002. Improving intrinsic water-use efficiency and crop yield. *Crop Science* **42**, 122–131.
- Condon AG, Richards RA, Rebetzke GJ, Farquhar GD.** 2004. Breeding for high water-use efficiency. *Journal of Experimental Botany* **55**, 2447–2460.
- Deery DM, Rebetzke GJ, Jimenez-Berni JA, Bovill WD, James RA, Condon AG, Furbank RT, Chapman SC, Fischer RA.** 2019. Evaluation of the phenotypic repeatability of canopy temperature in wheat using continuous-terrestrial and airborne measurements. *Frontiers in Plant Science* **10**, 875.
- Deery DM, Rebetzke GJ, Jimenez-Berni JA, James RA, Condon AG, Bovill WD, Hutchinson P, Scarrow J, Davy R, Furbank RT.** 2016. Methodology for high-throughput field phenotyping of canopy temperature using airborne thermography. *Frontiers in Plant Science* **7**, 1808.
- De Kort H, Panis B, Helsen K, Douzet R, Janssens SB, Honnay O.** 2020. Pre-adaptation to climate change through topography-driven phenotypic plasticity. *Journal of Ecology* **108**, 1465–1474.
- Delgado D, Sánchez-Bermejo E, de Marcos A, Martín-Jimenez C, Fenoll C, Alonso-Blanco C, Mena M.** 2019. A genetic dissection of natural variation for stomatal abundance traits in *Arabidopsis*. *Frontiers in Plant Science* **10**, 1392.
- Des Marais DL, Hernandez KM, Juenger TE.** 2013. Genotype-by-environment interaction and plasticity: exploring genomic responses of plants to the abiotic environment. *Annual Review of Ecology, Evolution, and Systematics* **44**, 5–29.
- Devos KM, Wang Z, Beales J, Sasaki T, Gale M.** 1998. Comparative genetic maps of foxtail millet (*Setaria italica*) and rice (*Oryza sativa*). *Theoretical and Applied Genetics* **96**, 63–68.
- Dillen SY, Marron N, Koch B, Ceulemans R.** 2008. Genetic variation of stomatal traits and carbon isotope discrimination in two hybrid poplar families (*Populus deltoides* ‘S9-2’ × *P. nigra* ‘Ghoy’ and *P. deltoides* ‘S9-2’ × *P. trichocarpa* ‘V24’). *Annals of Botany* **102**, 399–407.
- Dittberner H, Korte A, Mettler-Altmann T, Weber APM, Monroe G, de Meaux J.** 2018. Natural variation in stomata size contributes to the local adaptation of water-use efficiency in *Arabidopsis thaliana*. *Molecular Ecology* **27**, 4052–4065.
- Dow GJ, Bergmann DC.** 2014. Patterning and processes: how stomatal development defines physiological potential. *Current Opinion in Plant Biology* **21**, 67–74.
- Ellsworth PZ, Feldman MJ, Baxter I, Cousins AB.** 2020. A genetic link between leaf carbon isotope composition and whole-plant water use efficiency in the C<sub>4</sub> grass *Setaria*. *The Plant Journal* **102**, 1234–1248.
- Faralli M, Matthews J, Lawson T.** 2019. Exploiting natural variation and genetic manipulation of stomatal conductance for crop improvement. *Current Opinion in Plant Biology* **49**, 1–7.
- Farquhar G, Hubick K, Condon A, Richards R.** 1989. Carbon isotope fractionation and plant water-use efficiency. In: Rundel PW, Ehleringer JR, Nagy KA, eds. *Stable isotopes in ecological research*. New York: Springer, 21–40.
- Feldman MJ, Ellsworth PZ, Fahlgren N, Gehan MA, Cousins AB, Baxter I.** 2018. Components of water use efficiency have unique genetic signatures in the model C<sub>4</sub> grass *Setaria*. *Plant Physiology* **178**, 699–715.
- Feldman MJ, Paul RE, Banan D, et al.** 2017. Time dependent genetic analysis links field and controlled environment phenotypes in the model C<sub>4</sub> grass *Setaria*. *PLoS Genetics* **13**, e1006841.
- Fetter KC, Eberhardt S, Barclay RS, Wing S, Keller SR.** 2019. StomataCounter: a neural network for automatic stomata identification and counting. *New Phytologist* **223**, 1671–1681.
- Fischer R, Rees D, Sayre K, Lu ZM, Condon A, Saavedra AL.** 1998. Wheat yield progress associated with higher stomatal conductance and photosynthetic rate, and cooler canopies. *Crop Science* **38**, 1467–1475.
- Gailing O, Langenfeld-Heyser R, Polle A, Finkeldey R.** 2008. Quantitative trait loci affecting stomatal density and growth in a *Quercus robur* progeny: implications for the adaptation to changing environments. *Global Change Biology* **14**, 1934–1946.
- Gray SB, Dermody O, Klein SP, et al.** 2016. Intensifying drought eliminates the expected benefits of elevated carbon dioxide for soybean. *Nature Plants* **2**, 16132.
- Hall N, Griffiths H, Corlett J, Jones H, Lynn J, King G.** 2005. Relationships between water-use traits and photosynthesis in *Brassica oleracea* resolved by quantitative genetic analysis. *Plant Breeding* **124**, 557–564.
- Hamdy A, Ragab R, Scarascia-Mugnozza E.** 2003. Coping with water scarcity: water saving and increasing water productivity. *Irrigation and Drainage* **52**, 3–20.
- Haus MJ, Kelsch RD, Jacobs TW.** 2015. Application of optical topometry to analysis of the plant epidermis. *Plant Physiology* **169**, 946–959.
- Hetherington AM, Woodward FI.** 2003. The role of stomata in sensing and driving environmental change. *Nature* **424**, 901–908.
- Jones HG.** 1977. Transpiration in barley lines with differing stomatal frequencies. *Journal of Experimental Botany* **28**, 162–168.
- Jones HG.** 2004. Application of thermal imaging and infrared sensing in plant physiology and ecophysiology. *Advances in Botanical Research* **41**, 107–163.
- Khazaei H, Mohammady S, Monneveux P, Stoddard F.** 2011. The determination of direct and indirect effects of carbon isotope discrimination ( $\Delta$ ), stomatal characteristics and water use efficiency on grain yield in wheat using sequential path analysis. *Australian Journal of Crop Science* **5**, 466.
- Khazaei H, O’Sullivan DM, Sillanpää MJ, Stoddard FL.** 2014. Use of synteny to identify candidate genes underlying QTL controlling stomatal traits in faba bean (*Vicia faba* L.). *Theoretical and Applied Genetics* **127**, 2371–2385.
- Kholová J, Hash CT, Kakkera A, Kocová M, Vadez V.** 2010. Constitutive water-conserving mechanisms are correlated with the terminal drought tolerance of pearl millet [*Pennisetum glaucum* (L.) R. Br.]. *Journal of Experimental Botany* **61**, 369–377.
- Kimura Y, Aoki S, Ando E, et al.** 2015. A flowering integrator, SOC1, affects stomatal opening in *Arabidopsis thaliana*. *Plant & Cell Physiology* **56**, 640–649.
- Kulya C, Siangliwb JL, Toojindab T, Lontoma W, Pattanagula W, Sriyota N, Sanitchon J, Theerakulpisuta P.** 2018. Variation in leaf anatomical characteristics in chromosomal segment substitution lines of KDML105 carrying drought tolerant QTL segments. *ScienceAsia* **44**, 197–211.
- Kwak IY, Moore CR, Spalding EP, Broman KW.** 2014. A simple regression-based method to map quantitative trait loci underlying functional phenotypes. *Genetics* **197**, 1409–1416.

- Laza MRC, Kondo M, Ideta O, Barlaan E, Imbe T.** 2010. Quantitative trait loci for stomatal density and size in lowland rice. *Euphytica* **172**, 149–158.
- Leakey ADB, Ferguson JN, Pignon CP, Wu A, Jin Z, Hammer GL, Lobell DB.** 2019. Water use efficiency as a constraint and target for improving the resilience and productivity of C<sub>3</sub> and C<sub>4</sub> crops. *Annual Review of Plant Biology* **70**, 781–808.
- Li K, Huang J, Song W, Wang J, Lv S, Wang X.** 2019. Automatic segmentation and measurement methods of living stomata of plants based on the CV model. *Plant Methods* **15**, 67.
- Li P, Brutnell TP.** 2011. *Setaria viridis* and *Setaria italica*, model genetic systems for the Panicoideae grasses. *Journal of Experimental Botany* **62**, 3031–3037.
- Liao JX, Chang J, Wang GX.** 2005. Stomatal density and gas exchange in six wheat cultivars. *Cereal Research Communications* **33**, 719–726.
- Liu X, Fan Y, Mak M, et al.** 2017. QTL for stomatal and photosynthetic traits related to salinity tolerance in barley. *BMC Genomics* **18**, 9.
- Liu Y, Subhash C, Yan J, Song C, Zhao J, Li J.** 2011. Maize leaf temperature responses to drought: thermal imaging and quantitative trait loci (QTL) mapping. *Environmental and Experimental Botany* **71**, 158–165.
- Lu J, He J, Zhou X, Zhong J, Li J, Liang YK.** 2019. Homologous genes of epidermal patterning factor regulate stomatal development in rice. *Journal of Plant Physiology* **234–235**, 18–27.
- Martre P, Cochard H, Durand JL.** 2001. Hydraulic architecture and water flow in growing grass tillers (*Festuca arundinacea* Schreb.). *Plant, Cell & Environment* **24**, 65–76.
- Mason RE, Hays DB, Mondal S, Ibrahim AM, Basnet BR.** 2013. QTL for yield, yield components and canopy temperature depression in wheat under late sown field conditions. *Euphytica* **194**, 243–259.
- Mauro-Herrera M, Doust AN.** 2016. Development and genetic control of plant architecture and biomass in the panicoideae grass, *Setaria*. *PLoS One* **11**, e0151346.
- Mohammed U, Caine RS, Atkinson JA, Harrison EL, Wells D, Chater CC, Gray JE, Swarup R, Murchie EH.** 2019. Author Correction: rice plants overexpressing OsEPF1 show reduced stomatal density and increased root cortical aerenchyma formation. *Scientific Reports* **9**, 14827.
- Morison JI, Baker NR, Mullineaux PM, Davies WJ.** 2007. Improving water use in crop production. *Philosophical Transactions of the Royal Society B: Biological Sciences* **363**, 639–658.
- Nakashima K, Takasaki H, Mizoi J, Shinozaki K, Yamaguchi-Shinozaki K.** 2012. NAC transcription factors in plant abiotic stress responses. *Biochimica et Biophysica Acta* **1819**, 97–103.
- Nelson DE, Repetti PP, Adams TR, et al.** 2007. Plant nuclear factor Y (NF-Y) B subunits confer drought tolerance and lead to improved corn yields on water-limited acres. *Proceedings of the National Academy of Sciences, USA* **104**, 16450–16455.
- Nemali KS, Bonin C, Dohleman FG, et al.** 2015. Physiological responses related to increased grain yield under drought in the first biotechnology-derived drought-tolerant maize. *Plant, Cell & Environment* **38**, 1866–1880.
- Nunes TDG, Zhang D, Raissig MT.** 2020. Form, development and function of grass stomata. *The Plant Journal* **101**, 780–799.
- Ohsumi A, Kanemura T, Homma K, Horie T, Shiraiwa T.** 2007. Genotypic variation of stomatal conductance in relation to stomatal density and length in rice (*Oryza sativa* L.). *Plant Production Science* **10**, 322–328.
- Prado SA, Cabrera-Bosquet L, Grau A, Coupel-Ledru A, Millet EJ, Welcker C, Tardieu F.** 2018. Phenomics allows identification of genomic regions affecting maize stomatal conductance with conditional effects of water deficit and evaporative demand. *Plant, Cell & Environment* **41**, 314–326.
- Prakash PT, Banan D, Paul RE, Feldman MJ, Xie D, Freyfogle L, Baxter I, Leakey ADB.** 2021. Data from: Correlation and co-localization of QTL for stomatal density, canopy temperature, and productivity with and without drought stress in *Setaria*. *Journal of Experimental Botany* **72**, XXX–XXX.
- Raissig MT, Matos JL, Anleu Gil MX, et al.** 2017. Mobile MUTE specifies subsidiary cells to build physiologically improved grass stomata. *Science* **355**, 1215–1218.
- Rowland-Bamford AJ, Nordenbrock C, Baker JT, Bowes G, Allen LH Jr.** 1990. Changes in stomatal density in rice grown under various CO<sub>2</sub> regimes with natural solar irradiance. *Environmental and Experimental Botany* **30**, 175–180.
- Sagan V, Maimaitijiang M, Sidike P, Eblimit K, Peterson KT, Hartling S, Esposito F, Khanal K, Newcomb M, Pauli D.** 2019. UAV-based high resolution thermal imaging for vegetation monitoring, and plant phenotyping using ICI 8640 P, FLIR Vue Pro R 640, and thermomap cameras. *Remote Sensing* **11**, 330.
- Schoppach R, Taylor JD, Majerus E, Claverie E, Baumann U, Suchecki R, Fleury D, Sadok W.** 2016. High resolution mapping of traits related to whole-plant transpiration under increasing evaporative demand in wheat. *Journal of Experimental Botany* **67**, 2847–2860.
- Shahinnia F, Le Roy J, Laborde B, Sznajder B, Kalambettu P, Mahjourimajd S, Tilbrook J, Fleury D.** 2016. Genetic association of stomatal traits and yield in wheat grown in low rainfall environments. *BMC Plant Biology* **16**, 150.
- Sinclair TR, Devi J, Shekoofa A, Choudhary S, Sadok W, Vadez V, Riar M, Ruffy T.** 2017. Limited-transpiration response to high vapor pressure deficit in crop species. *Plant Science* **260**, 109–118.
- Stocker TF, Qin D, Plattner GK, Tignor M, Allen SK, Boschung J, Nauels A, Xia Y, Bex V, Midgley PM.** 2013. *Climate change 2013: the physical science basis*. Cambridge: Cambridge University Press.
- Tardieu F.** 2013. Plant response to environmental conditions: assessing potential production, water demand, and negative effects of water deficit. *Frontiers in Physiology* **4**, 17.
- Turner NC, Wright GC, Siddique K.** 2001. Adaptation of grain legumes (pulses) to water-limited environments. *Advances in Agronomy* **71**, 193–231.
- Valliyodan B, Nguyen HT.** 2006. Understanding regulatory networks and engineering for enhanced drought tolerance in plants. *Current Opinion in Plant Biology* **9**, 189–195.
- Violet-Chabrand S, Lawson T.** 2019. Dynamic leaf energy balance: deriving stomatal conductance from thermal imaging in a dynamic environment. *Journal of Experimental Botany* **70**, 2839–2855.
- Wang Z, Devos K, Liu C, Wang R, Gale M.** 1998. Construction of RFLP-based maps of foxtail millet, *Setaria italica* (L.) P. Beauv. *Theoretical and Applied Genetics* **96**, 31–36.
- Wang SG, Jia SS, Sun DZ, Hua F, Chang XP, Jing RL.** 2016. Mapping QTL for stomatal density and size under drought stress in wheat (*Triticum aestivum* L.). *Journal of Integrative Agriculture* **15**, 1955–1967.
- White T, Snow V.** 2012. A modelling analysis to identify plant traits for enhanced water-use efficiency of pasture. *Crop and Pasture Science* **63**, 63–76.
- Wickham H.** 2016. *Ggplot2: elegant graphics for data analysis*. New York: Springer-Verlag.
- Xie X, Mayfield-Jones D, Erice G, Choi M, Leakey ADB.** 2020. Optical topometry and machine learning to rapidly phenotype stomatal patterning traits for QTL mapping in maize. *BioRxiv* doi: [10.1101/2020.10.09.333880v1](https://doi.org/10.1101/2020.10.09.333880v1) [Preprint].
- Xu Z, Zhou G.** 2008. Responses of leaf stomatal density to water status and its relationship with photosynthesis in a grass. *Journal of Experimental Botany* **59**, 3317–3325.
- Zhang JZ, Creelman RA, Zhu JK.** 2004. From laboratory to field. Using information from Arabidopsis to engineer salt, cold, and drought tolerance in crops. *Plant Physiology* **135**, 615–621.